

Evolution of Stress Along the Southern San Andreas Fault System for the Past Two Centuries

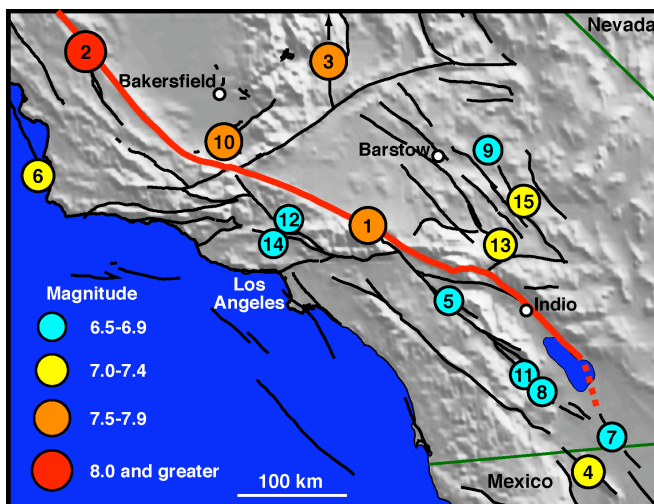
Award No. 03HQGR0082

Andrew Freed
Dept. of Earth & Atmospheric Sciences
Purdue University
550 Stadium Mall Drive
West Lafayette, IN 47907-2051
Phone: (765)496-3738
Fax: (765) 496-1210
freed@purdue.edu

Roland Bürgmann
Department of Earth & Planetary Science
University of California
389 McCone Hall
Berkeley, CA 94720
Phone (510) 643-9545
Fax (510) 643-9980
burgmann@seismo.berkeley.edu

Project Overview

The objective of our project is to calculate the evolution of stress along the southern San Andreas fault and surrounding regions during the past two centuries in order to indicate which regions have had the most dramatic buildup of unreleased stress to date, potentially indicating where the next major earthquakes are most likely to occur. We will use a 3-D, viscoelastic finite element model that will span the whole width of the southern San Andreas fault system south of Parkfield. The model will calculate stress changes due to all major ($M_w > 6.5$) southern California earthquakes for the past 200 years (Figure 1) and associated postseismic viscous flow, and stress evolution due to the relative motions of the North American and Pacific plates and aseismic slip on creeping portions of the San Andreas fault. Most important for a long-term viscous calculation, the model will include a geodetically, geologically, thermally, and laboratory constrained, temperature dependent, powerlaw viscosity structure (strain rate proportional to stress raised to a power) in order to reduce errors associated with the more common assumption of a nearly homogeneous Newtonian viscosity structure.



No.	Year	Magnitude	Location
1.	1812	$M_w = 7.5$	Wrightwood
2.	1857	$M_w = 8.0$	Fort Tejon
3.	1872	$M_w = 7.8$	Owens Valley
4.	1892	$M_w = 7.0$	Laguna Salada
5.	1918	$M_w = 6.8$	San Jacinto
6.	1927	$M_w = 7.3$	Lompoc
7.	1940	$M_w = 6.9$	Imperial Valley
8.	1942	$M_w = 6.6$	Fish Creek Mnts
9.	1947	$M_w = 6.5$	Manix
10.	1952	$M_w = 7.5$	Kern County
11.	1968	$M_w = 6.5$	Borrego Mountain
12.	1971	$M_w = 6.6$	San Fernando
13.	1992	$M_w = 7.3$	Landers
14.	1994	$M_w = 6.7$	Northridge
15.	1999	$M_w = 7.1$	Hector Mine

Interim Project Status

We have recently completed two preliminary studies, the first sought to understand the influence of the Mojave earthquake sequence (1992 Joshua Tree, Landers, Big Bear, and 1999 Hector Mine) and subsequent postseismic deformation on the stress field in southern California as a function of time. We began our investigation with these modern events as they are best constrained, enabling us to better develop modeling techniques that will be required for the less well constrained historic events. An important finding of this study was that viscous relaxation appears to take place primarily in the upper mantle and that such relaxation is currently loading the San Bernardino segment of the southern San Andreas Fault. Figure 1 below shows the projected influence of the Mojave sequence on southern California, shown as Coulomb stress changes for faults oriented parallel to the San Andreas fault through San Bernardino.

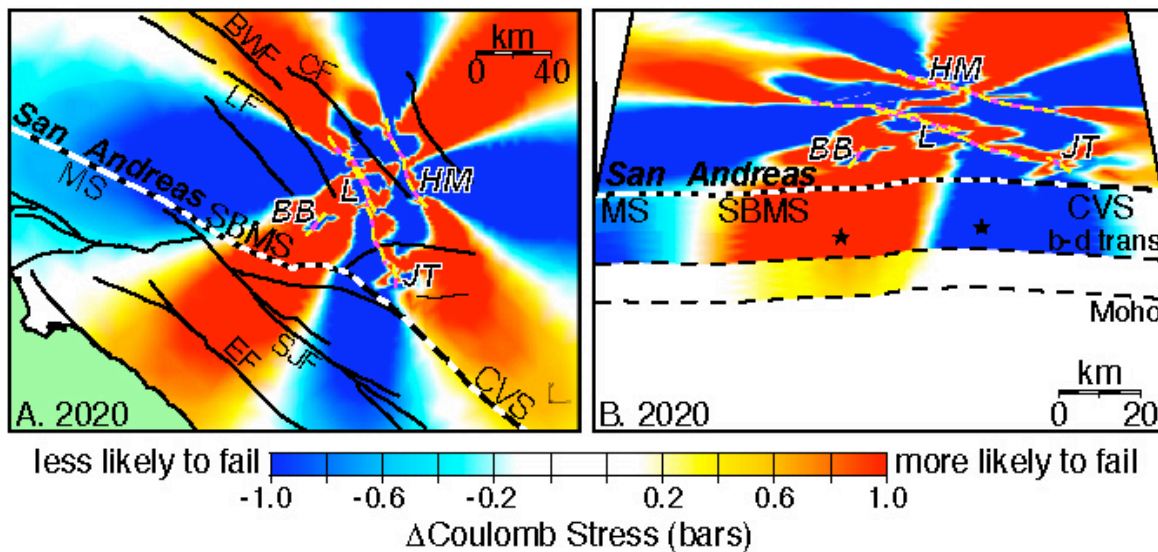


Figure 2. Calculated coseismic + postseismic Coulomb stress changes through the year 2020 caused by the 1992 Joshua Tree (JT), Landers (L), and Big Bear (BB), and 1999 Hector Mine earthquakes (yellow/purple lines). A. Map view. B. Cut plane along the San Andreas fault. Other faults: MS—Mojave segment, SBMS—San Bernardino Mountain segment, and CVS—Coachella Valley segment of San Andreas fault; SJF—San Jacinto fault, EF—Elsinore fault, CF—Calico fault, LF—Lenwood, and BWF—Blackwater fault. Receiver faults for Coulomb stress calculations shown are assumed to strike N60°W with an apparent friction coefficient $\mu = 0.2$.

We also completed a second study in which we sought to ascertain whether the viscous rheology beneath the Mojave Desert (and by extension all of southern California) behaves like a linear Maxwell solid or behaves following a powerlaw (as suggested by rock experiments). The linearity of the flow will influence how the rate of postseismic stress transfer changes in time following each event. Our results strongly suggest that the viscous rheology of the Mojave lithosphere behaves as a powerlaw material. This is illustrated in Figure 3, which shows that a single powerlaw model can explain the post-Landers and post-Hector Mine time-series transients, while two Newtonian models (one with a viscosity an order of magnitude higher than the other) are required to explain the same data.

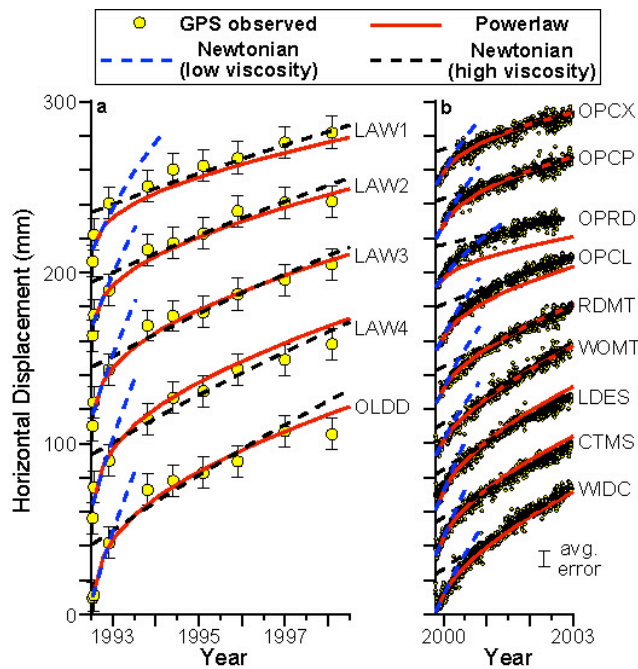


Figure 3. Comparison of representative observed and calculated postseismic displacement time-series. (a) Horizontal displacements at 5 campaign GPS stations following the 1992 Landers quake. (b) Horizontal surface displacements at 9 continuously monitored GPS stations following 1999 Hector Mine earthquake. Powerlaw mantle flow model (solid red curves) is model 8 in Figure 2 (aplite, wet olivine, $T_{40\text{ km}} = 1225\text{ }^{\circ}\text{C}$; powerlaw parameters listed in Table 1). Newtonian models consider predominately mantle flow with low viscosity ($2.5 \times 10^{18}\text{ Pa s}$, blue dashed curves) and an order of magnitude higher viscosity ($2.5 \times 10^{19}\text{ Pa s}$, black dashed curves) that match early and late time-series slopes, respectively. Curves associated with the low viscosity Newtonian model have been raised to show where the slopes match the observed time-series.

With the completion of these preliminary analyses, we are now beginning to assemble our full model of southern California. The initial tasks include collecting all data relevant to understanding the rupture geometry, inferred slip distributions, and associated uncertainty of the historic events, and beginning to assemble a regional model of North America/Pacific Plate motion that contributed to regional stress rates (this model will be calibrated to the SCEC velocity field). Once this phase is completed we will begin calculations of the evolution of stress due to historic seismicity and the regional strain rate.